Available *online* at: https://dergipark.org.tr/en/pub/jster

Journal of Science, Technology and Engineering Research

| ISSN (Online) 2717-8404 |

Research Article DOI: 10.53525/jster.1892489

Comparison of Distance and Physical Obstacle Effects on Real-Time Data Transmission Using Esp32 and LoRa

Cafer Ayhan KOLCU[1]
Reşat Özgür DORUK[2]

[1] Atılım University, Department of Electrical and Electronic Engineering, 06830 İncek, Gölbaşı, Ankara/TURKEY
kolcu.caferayhan@student.atilim.edu.tr, Orcid.0009-0001-6560-8696
[2] Atılım University, Department of Electrical and Electronic Engineering, 06830 İncek, Gölbaşı, Ankara/TURKEY
resat.doruk@atilim.edu.tr, Orcid.0000-0002-9217-0845

HIGHLIGHTS

- ESP32 and LoRa comparison
- Indoor RSSI performance analysis
- Obstacle-based signal attenuation
- Corridor-based environment measurements
- Experimental biomedical data transmission

ARTICLE INFORMATION

Received Date February 18, 2026
Accepted Date April 24, 2026
Publication Date April 29, 2026

Corresponding author:

Cafer Ayhan KOLCU
E-mail: ayhankolcu@gmail.com

Cite this article:
Kolcu, C. A., Doruk, R. Ö. (2026). Comparison of Distance and Physical Obstacle Effects on Real-Time Data Transmission Using ESP32 and LoRa, Journal of Science, Technology and Engineering Research, (1):(2026).
DOI: 10.53525/jster.1892489

ABSTRACT

Reliable indoor real-time data transmission is essential for biomedical and IoT monitoring applications; however, wireless link quality can vary significantly with distance and the presence of common building materials. This study presents an experimental comparison of ESP32-based Wi-Fi (2.4 GHz) and LoRa RA-02 communication (433 MHz) under indoor conditions, with a focus on the effects of propagation distance and physical obstacles on link performance. In addition to communication analysis, the study also demonstrates the acquisition of analog biomedical signals and environmental data, their wireless transmission, and real-time visualization at the receiver side. To ensure a consistent comparison, both technologies were tested under identical indoor procedures using received signal strength indicator (RSSI) as the primary evaluation metric. Four experimental scenarios were considered, including short-range reference measurement, straight-corridor distance tests, non-line-of-sight L-shaped corridor measurements, and obstacle-based attenuation tests involving commonly encountered construction materials. The experimental results show that ESP32-based Wi-Fi provides satisfactory performance in short-range and relatively unobstructed indoor environments, where higher data exchange capability is advantageous. However, its signal strength decreases more noticeably as transmission distance increases and when obstacles are introduced. In contrast, LoRa exhibits greater resistance to attenuation caused by both distance and indoor obstacles, maintaining more stable RSSI behavior across medium- and longer-range scenarios. Overall, the study provides a practical indoor performance evaluation of two widely used wireless communication technologies and demonstrates that protocol selection should not depend solely on nominal communication range, but also on obstacle sensitivity and application-specific monitoring requirements. The findings offer useful guidance for the design of indoor biomedical and IoT monitoring systems operating in realistic built environments.

Keywords: ESP32, LoRa, Indoor Wireless Communication, Obstacle Attenuation, Biomedical Data Transmission

I. INTRODUCTION

Recent advances in embedded systems and the widespread availability of low-cost wireless modules have significantly facilitated real-time data acquisition from physical and biomedical environments. Wireless communication technologies, in particular, enable compact and modular monitoring systems capable of operating under practical indoor conditions. Among the commonly used options, Wi-Fi-based solutions and sub-GHz long-range technologies are preferred due to their accessibility and integration convenience in IoT-oriented designs [1].

Indoor wireless communication remains challenging because signal propagation is strongly influenced by distance, obstructions, and material properties. As carrier frequency increases, signals typically become more sensitive to attenuation and shadowing effects, which can degrade link reliability in multi-room and obstacle-rich environments. Wi-Fi-based platforms such as ESP32 are therefore often used in short-range or same-room scenarios, whereas sub-GHz technologies such as LoRa are frequently considered more robust for longer distances or non-line-of-sight conditions due to their lower operating frequency [4], [14].

In biomedical and health-monitoring contexts, these propagation effects become particularly important because reliable data delivery is essential for continuous observation and timely decision-making. A practical monitoring system often requires both real-time visualization and stable transmission performance under indoor constraints. Accordingly, this study investigates two wireless communication technologies -ESP32-based Wi-Fi at 2.4 GHz and the LoRa RA-02 module at 433 MHz- within a transmitter–receiver architecture designed for indoor measurement and monitoring. The transmitter unit acquires temperature and humidity data using a DHT22 sensor and biomedical pulse-related signals using an AD8232 analog front-end module, while the receiver unit visualizes sensor readings and RSSI values in real time on a 1.3-inch ST7789 TFT display (240 × 240 pixels) [6].

Although latency and data transmission rate were also observed during system operation, they were not used as the primary comparison metrics in this study. Since the LoRa-based configuration employed a fixed 200 ms packet transmission interval, RSSI provided a more direct and consistent basis for comparing the effects of distance and physical obstacles under identical indoor conditions.

In this context, the main contribution of this work is an experimental comparison of ESP32 and LoRa RSSI behavior under controlled and repeatable indoor scenarios**.** The study evaluates distance-dependent attenuation and obstacle-induced effects using multiple indoor measurement configurations, with repeated sampling to support stable comparisons. The contributions of this study can be summarized as follows:

- A controlled indoor experimental framework for comparing ESP32 (2.4 GHz) and LoRa (433 MHz) RSSI performance under identical conditions.
- Distance-based evaluation of RSSI trends for both technologies across multiple indoor ranges.
- Obstacle-based evaluation using commonly encountered building and furnishing materials, highlighting how material characteristics influence RSSI behavior.
- A practical monitoring-oriented system setup that supports real-time visualization of sensor data and RSSI values, enabling technology selection insights for indoor biomedical/IoT applications.

Overall, the results provide guidance for selecting appropriate wireless technologies depending on indoor distance requirements, obstacle density, and reliability constraints, and they offer an experimentally grounded reference for future indoor propagation and monitoring system studies.

II. METHOD AND PROCEDURE

Two hardware circuits were designed and implemented for this study: a transmitter unit and a receiver unit. The overall system architecture was developed to acquire analog and digital signals from real-world biomedical and environmental sources and to transmit these data wirelessly under indoor conditions using two different communication technologies. The receiver and transmitter circuit schematics are presented in Figure 1 and Figure 2, respectively.

 https://doi.org/10.53525/jster.1892489

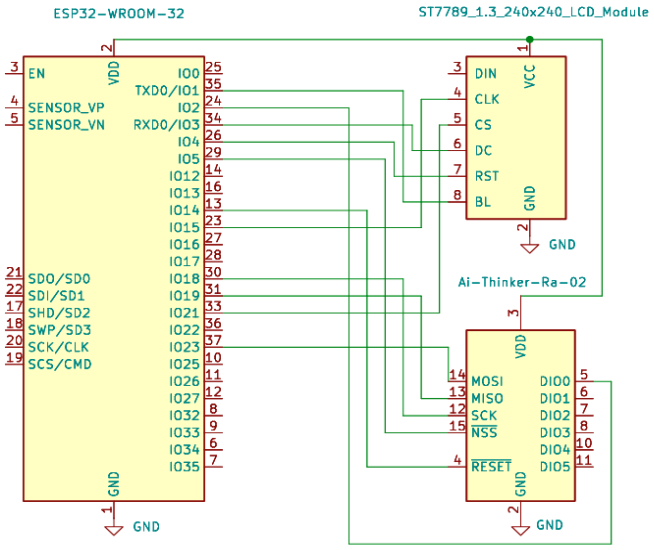

Figure 1. Receiver Circuit Schematic
(ESP32 – LoRa – ST7789)

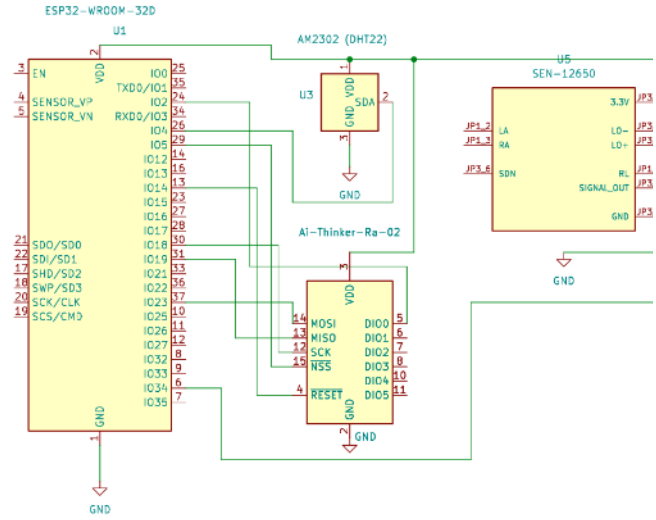

Figure 2. Transmitter Circuit Schematic
(ESP32 – LoRa – DHT22 – AD8232)

2.1. Transmitter Unit

The transmitter circuit was designed to collect sensor data and transmit the processed information wirelessly. Temperature and humidity measurements were obtained using a DHT22 sensor, while biomedical pulse signals were acquired through an AD8232 analog front-end module [10], [12]. These analog signals were digitized using an ESP32-based microcontroller [2], which performed the necessary signal conditioning and packet formation prior to transmission. Depending on the selected communication mode, the data packets were transmitted either via the ESP32's integrated 2.4 GHz Wi-Fi interface or through a LoRa RA-02 module operating at 433 MHz [7], [9]. The physical prototype of the transmitter circuit is presented in Figure 3.

Figure 3. Physical Prototype of the Transmitter Circuit

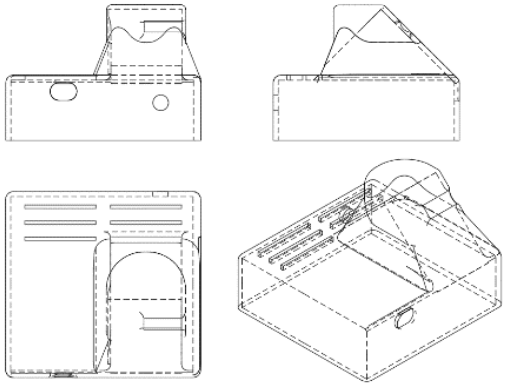

Figure 4. Technical Drawing of the Transmitter Enclosure

To ensure consistent and comparable measurements, sensor data were transmitted at predefined time intervals. This periodic transmission structure enabled reliable observation of received signal strength indicator (RSSI) values at the receiver side while maintaining stable communication behavior across different experimental scenarios. The technical drawing of the transmitter enclosure used to house the circuit components is shown in Figure 4.

2.2. Receiver Unit

The receiver circuit consisted of an ESP32 microcontroller interfaced with either Wi-Fi or LoRa communication modules, as well as a 1.3-inch ST7789 TFT display with a resolution of 240 × 240 pixels [13]. Incoming data packets were decoded by the microcontroller and visualized on the display, allowing real-time observation of sensor readings and RSSI values. This configuration facilitated continuous monitoring of wireless communication performance during the experiments. The physical prototype of the receiver circuit is presented in Figure 5, and the technical drawing of the receiver enclosure is shown in Figure 6.

https://doi.org/10.53525/jster.1892489

Figure 5. Physical Prototype of the Receiver Circuit

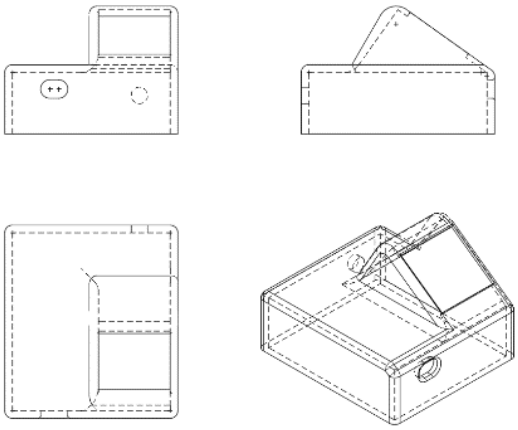

Figure 6. Technical Drawing of the Receiver Enclosure

2.3. Wireless Communication Characteristics

The two wireless technologies investigated in this study exhibit fundamentally different characteristics. ESP32-based Wi-Fi communication at 2.4 GHz provides higher data rates and is suitable for short-range indoor applications. However, it is more sensitive to distance and physical obstacles. In contrast, LoRa communication at 433 MHz offers lower data rates but demonstrates greater robustness and stability in obstacle-rich indoor environments due to its lower carrier frequency and propagation characteristics [14].

To obtain baseline theoretical reference values for the distance-dependent signal attenuation, the free-space path loss (FSPL) model was used. FSPL represents the ideal propagation loss between a transmitter and receiver under line-of-sight conditions in free space and is commonly used as a first-order reference in link-budget analyses.

The theoretical values computed with FSPL were used as baseline references for comparison with the measured RSSI trends under the same distance conditions.

2.4. Experimental Environment and Preliminary Tests

All experiments were conducted exclusively in indoor environments. Initial long-range tests revealed that signal reliability degraded significantly beyond certain distances; therefore, subsequent experiments were performed within optimized distance ranges to ensure stable communication. Additional preliminary tests demonstrated that the relative height and positioning of the transmitter and receiver units affected signal stability, with improved performance observed when both units were positioned centrally within the experimental environment.

Specific attention was given to corridor-based and L-shaped scenarios, where signal propagation involved direction changes and partial obstruction. In such cases, elements such as aluminium door frames and metallic structures were observed to cause noticeable signal attenuation. Furthermore, environmental factors including floor, wall, and ceiling materials influenced RSSI behavior. Based on these observations, experimental locations were carefully selected to minimize uncontrolled reflections and material-induced interference, allowing the measured results to align more closely with theoretical propagation expectations.

III. EXPERIMENTAL SCENARIOS

This section describes the experimental setups and the rationale behind their selection. All scenarios were designed to enable a fair and repeatable comparison between ESP32-based Wi-Fi and LoRa communication under identical indoor conditions. Each experiment was conducted using the same hardware, antenna configurations, transmission intervals, and measurement procedures for both communication technologies.

3.1. Experimental Setup and Repeatability

To ensure compatibility across different measurement scenarios, custom enclosures and holders were developed for the transmitter and receiver units. These holders were designed to protect the circuits from mechanical disturbances while minimizing any potential impact on antenna radiation characteristics. The lower profile of the enclosure provided mechanical stability without obstructing signal propagation.

 https://doi.org/10.53525/jster.1892489

All measurement scenarios were repeated for both ESP32 and LoRa communication. To guarantee that measurements were taken at precisely the same locations, reference markings were used at each contact point with the floor. This approach ensured that repositioning the devices -such as after code modifications or module changes- did not introduce positional bias. The same procedure was applied when adjusting distances or replacing physical obstacles between the transmitter and receiver. As a result, all experimental conditions were kept identical for both communication protocols, enabling a direct and reliable comparison.

All experiments were conducted in indoor environments. Measurements were performed with antenna orientations arranged to maintain line-of-sight (LOS) wherever applicable, unless the scenario explicitly involved directional changes or obstacle placement.

3.2. Scenario 1: Short-Distance Reference Measurement

The first experiment was conducted at a short distance of 30cm with the transmitter and receiver antennas facing each other. Measurements were carried out in an unobstructed indoor space with a width of approximately 4m and a ceiling height of 240cm. For each communication technology, five measurements were recorded over two-minute intervals, and average RSSI values were calculated. The results obtained from this scenario were used as reference values for subsequent experiments. The diagram and physical view of this experimental setup are presented in Figure 7 and Figure 8, respectively.

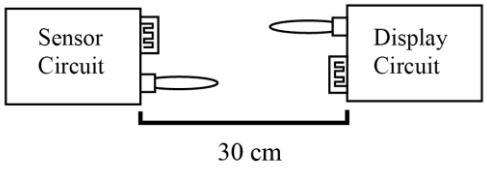

Figure 7. Diagram of Experimental Setup 1

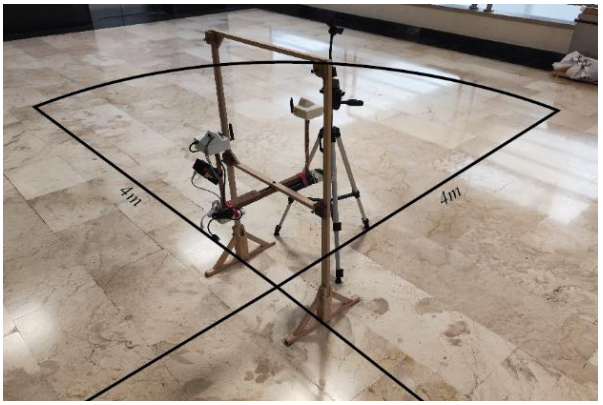

Figure 8. Experimental Setup 1 (Physical View)

3.3. Scenario 2: Straight Corridor Distance Measurements

The second experiment was performed in a straight corridor with a width of 360 cm and a height of 240 cm. The transmitter and receiver units were positioned at the geometric center of the corridor's width and height to reduce environmental asymmetry. Measurements were taken at three distances -5 m (near), 25 m (mid-range), and 50 m (far) - with five measurements recorded at each distance for both ESP32 and LoRa communication. The 5 m measurements served as reference values for the initial conditions of the third experimental scenario. The diagram of the second experimental setup is shown in Figure 9, while the physical measurement configurations for 5 m, 25 m, and 50 m are presented in Figure 10, Figure 11, and Figure 12, respectively.

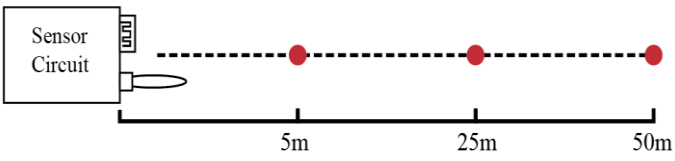

Figure 9 Diagram of Experimental Setup 2

https://doi.org/10.53525/jster.1892489

Figure 10. Setup 2: 5m Short-Range Measurement Scenario

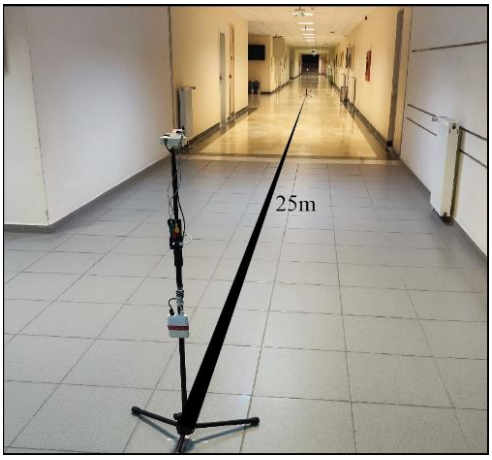

Figure 11. Setup 2: 25m Medium-Range Measurement Scenario

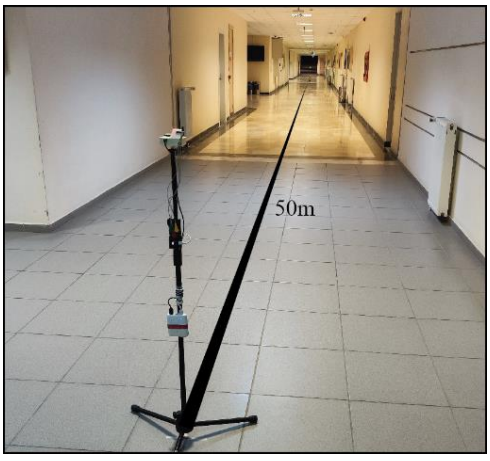

Figure 12. Setup 2: 50m Long-Range Measurement Scenario

3.4. Scenario 3: L-Shaped Corridor Measurements

The third experiment was conducted in an L-shaped corridor configuration to evaluate signal behavior under directional changes. The main corridor section measured approximately 5 m × 20 m, with measurement points incremented in 5 m steps. The transmitter unit was placed in a corridor section with a width of 520 cm and a height of 240 cm, and the initial measurement point was located 5 m directly opposite the transmitter. Subsequent measurements were obtained by moving the receiver unit along the perpendicular corridor section, which had a width of 360 cm and a height of 240 cm. Measurements were recorded up to a distance of 20 m, capturing the effects of non-line-of-sight (NLOS) propagation. The diagram of the L-shaped corridor measurement setup is shown in Figure 13.

The first measurement point, where the circuits were positioned directly facing each other with a separation distance of 5m, was defined as 0m(L). Subsequently, additional measurements were taken along the corridor at the following points:

- **5m(L):** 10m from the sensor circuit and 5m from the 0m(L) point.
- **10m(L):** 15m from the sensor circuit and 10m from the 0m(L) point.
- **15m(L):** 20m from the sensor circuit and 15m from the 0m(L) point.

The physical views of the measurement points at 0 m(L), 5 m(L), 10 m(L), and 15 m(L) are presented in Figure 14, Figure 15, Figure 16, and Figure 17, respectively. Since direct line of sight is absent at most points in this non-line-of-sight (NLOS) scenario, the effects of wall diffraction and multipath reflections on RSSI behavior and communication continuity were evaluated.

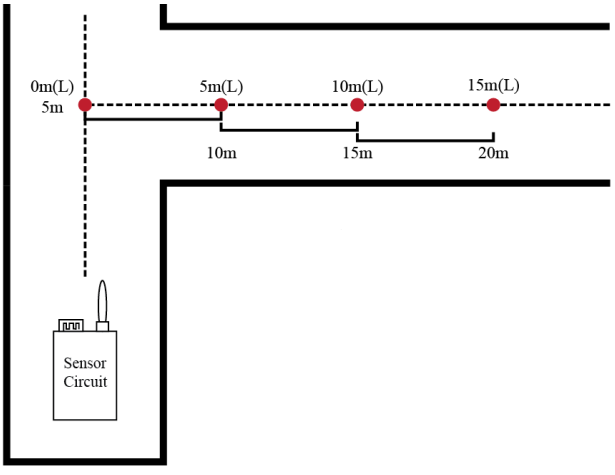

Figure 13. Diagram of Experimental Setup 3

 https://doi.org/10.53525/jster.1892489

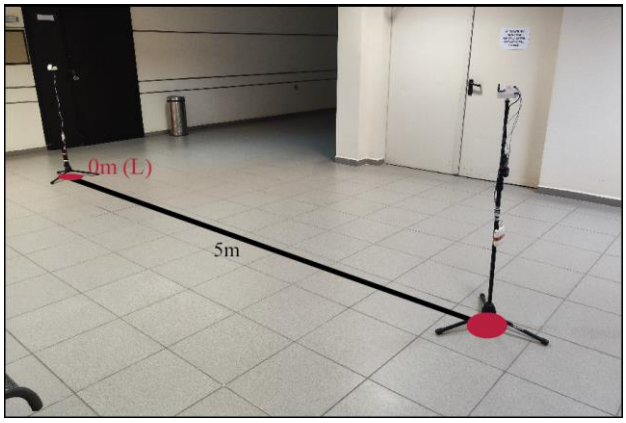

Figure 14. Setup 3: 0m(L) Point

Figure 15. Setup 3: 5m(L) Point

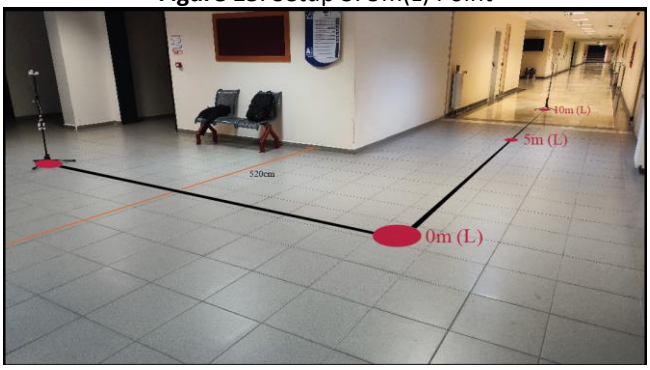

Figure 16. Setup 3: 10m(L) Point

Figure 17. Setup 3: 15m(L) Point

3.5. Scenario 4: Obstacle-Based Attenuation Measurements

The fourth experiment was conducted in the same environment as the short-distance reference scenario to isolate the effects of physical obstacles. Using the reference RSSI values obtained in Scenario 1, various obstacles were placed between the transmitter and receiver at a distance of 15 cm from the midpoint between the devices. Seven different obstacle materials were tested: stainless steel, aluminium composite, double-glazed glass, drywall, oriented strand board (OSB), particle board, and plexiglass. For each obstacle type, five measurements were recorded, and average RSSI values were calculated to evaluate material-dependent attenuation effects. The diagram of the obstacle-based experimental setup is shown in Figure 18, while the receiver-side view, transmitter-side view, and the tested obstacle materials are presented in Figure 19, Figure 20, and Figure 21, respectively.

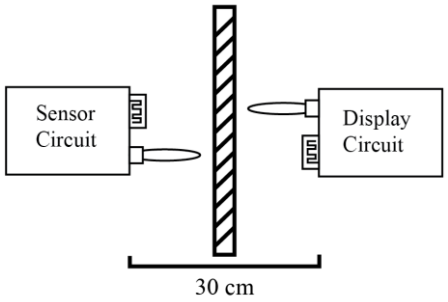

Figure 18. Diagram of Experimental Setup 4

Figure 19. Setup 4 and Obstacles (Receiver Side View)

https://doi.org/10.53525/jster.1892489

Figure 20. Setup 4 and Obstacles (Transmitter Side View)

Figure 21. Identification of the Obstacles Used in Experimental Setup 4

IV. FINDINGS AND RESULTS

The experimental results obtained for both communication protocols were recorded and comparatively analyzed. Overall, ESP32-based Wi-Fi communication exhibited more negative RSSI values than LoRa under identical conditions. For both technologies, RSSI values decreased as the transmission distance increased; however, the rate of degradation differed significantly between the two systems. In terms of latency, ESP32's high-throughput design provides a major advantage for real-time applications, while LoRa generates higher delays due to low data rates, longer packet durations, and duty-cycle constraints, consistent with prior studies [14]. Nevertheless, LoRa's long-range and low-power characteristics make it preferable in many remote monitoring scenarios, despite this latency disadvantage.

In the present prototype, this distinction was also reflected in the system design. Whereas ESP32 communication showed timing variations depending on instantaneous link quality, the LoRa-based structure was configured to transmit packetized data at fixed 200 ms intervals. Accordingly, the delay behavior observed in LoRa was influenced primarily by the predefined transmission cycle rather than solely by environmental channel variations. For this reason, although latency and transmission speed were monitored during operation, they were regarded as supplementary observations rather than the principal comparative metrics of the present analysis. ESP32 (2.4 GHz) – FSPL and RSSI

Assumptions:

- Frequency: 2400.0 MHz
- Transmitter and receiver antenna gains neglected (Gt = 0dBi, Gr = 0dBi)
- Environment: Free space; obstacles and multipath reflections neglected

Formulation:

The Free-Space Path Loss (FSPL) is given by:

$$FSPL(dB) = 20log_{10}(d) + 20log_{10}(f) + 20log_{10}\left(\frac{4\pi}{c}\right) \quad (2)$$

Where,

d is meaning of distance (m)
f is meaning of frequency (Hz)
c is meaning of speed of light (≈ 3×10⁸ m/s)

First Calculation (d = 30 cm)

d = 30 cm, f = 2400.0 MHz

$$FSPL(dB) = 20log_{10}(0{,}3) + 20log_{10}(2{,}4x10^{9}) + 20log_{10}\left(\frac{4\pi}{3x10^{8}}\right) \approx 29.59\ \text{dB}$$

RSSI (dBm) = -FSPL(dB) ≈ -29.59 dBm (3)

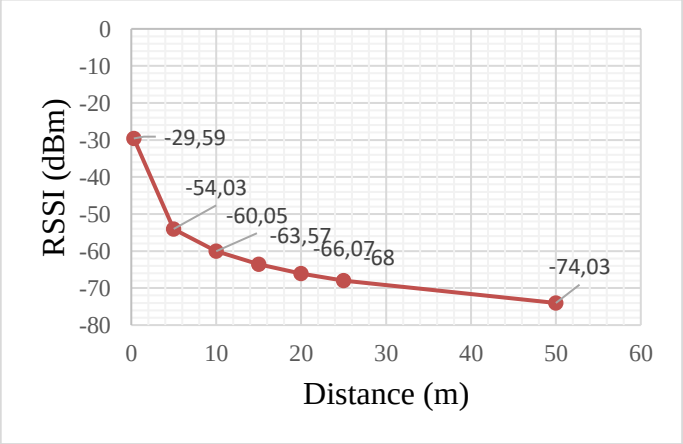

Figure 22. RSSI vs. Distance (Theoretical, ESP32)

Figure 22 illustrates the FSPL-based theoretical RSSI trend for ESP32 communication at 2.4 GHz as a function of distance. The predicted RSSI decreases sharply at short ranges, dropping from approximately −29.59 dBm at 30 cm to −54.03 dBm at 5 m, which reflects the rapid increase in path loss when moving from very close proximity to typical indoor operating distances. As distance increases further,

https://doi.org/10.53525/jster.1892489

the rate of decrease becomes more gradual, consistent with the logarithmic distance dependence of the FSPL model. For example, the theoretical RSSI is approximately −60.05 dBm at 10 m, −63.57 dBm at 15 m, −66.07 dBm at 20 m, and about −68 dBm at 25 m, indicating incremental losses of only a few dB over each additional 5 m step in this range. At 50 m, the predicted RSSI reaches approximately −74.03 dBm, and the overall trend shows that doubling the distance leads to an additional loss on the order of ~6 dB (e.g., 5–10 m and 25–50 m), which is characteristic of free-space propagation behavior.

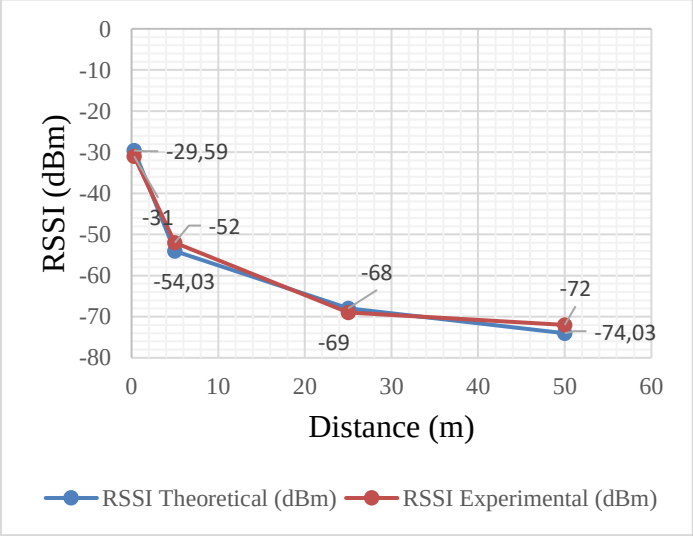

Figure 23. Theoretical vs. Experimental RSSI Comparison for ESP32

Figure 23 compares the theoretical (FSPL-based) and experimental RSSI values for ESP32 at 2.4 GHz across increasing distances. Both curves exhibit the same overall behavior: RSSI decreases rapidly at short distances and then declines more gradually as distance increases, which is consistent with the logarithmic distance dependence predicted by the FSPL model. At 30 cm, the theoretical RSSI is approximately −29.59 dBm while the experimental value is close to −31 dBm, indicating very good agreement at the reference short range. At 5 m, the theoretical prediction is −54.03 dBm and the measured RSSI is around −52 dBm, again showing a small deviation of only a few dB. At 25 m, the theoretical value is approximately −69 dBm and the experimental measurement is about −68 dBm, demonstrating near-overlap between the curves at mid-range distances. At 50 m, the theoretical RSSI is approximately −74.03 dBm, whereas the experimental value is around −72 dBm, meaning the measured signal remains slightly stronger than the theoretical baseline by roughly 1–2 dB. Overall, the close alignment between the theoretical and experimental curves suggests that distance-dependent attenuation in this scenario follows the expected free-space trend, while small deviations can be attributed to indoor environmental factors such as reflections and multipath propagation.

LoRa RA-02 (433 MHz) – FSPL and RSSI

Assumptions:

- Frequency: 433.0 MHz
- Transmitter and receiver antenna gains neglected (Gt = 0dBi, Gr = 0dBi)
- Environment: Free space; obstacles and multipath reflections neglected

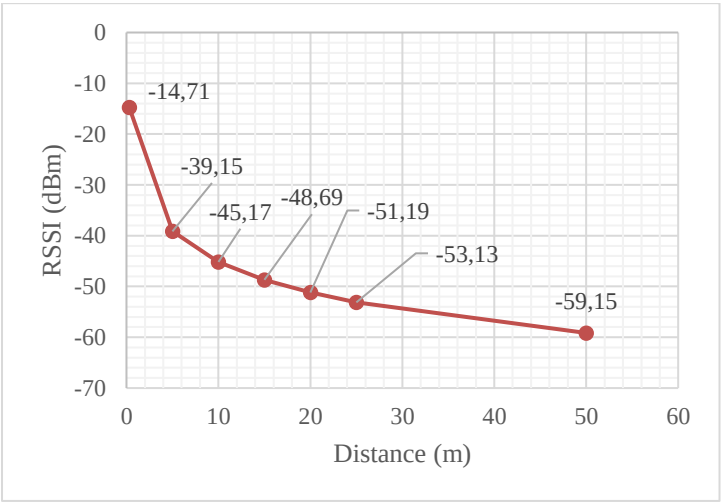

Figure 24. RSSI vs. Distance (Theoretical, LoRa)

Figure 24 presents the FSPL-based theoretical RSSI trend for LoRa communication at 433 MHz as a function of distance. Similar to the ESP32 case, the curve follows a logarithmic decay pattern, where the RSSI decreases rapidly at short ranges and then gradually flattens as distance increases. At 30 cm, the theoretical RSSI is approximately −14.71 dBm, indicating a strong received signal at very close proximity.

https://doi.org/10.53525/jster.1892489

As distance increases to 5 m and 10 m, the RSSI drops to roughly −39.15 dBm and −45.17 dBm, respectively, showing the largest attenuation occurring in the near-field-to-short-range transition. Beyond this region, the decrease becomes more incremental: the theoretical RSSI is about −48.69 dBm at 15 m, −51.19 dBm at 25 m, and approximately −53.13 dBm around 30 m, reflecting smaller additional losses per distance step. At 50 m, the predicted RSSI reaches approximately −59.15 dBm, and the overall trend is consistent with the expected ~6 dB reduction for distance doubling at longer ranges (e.g., 25–50 m). This theoretical behavior provides a baseline reference for evaluating the experimentally observed LoRa RSSI performance under the same distance conditions.

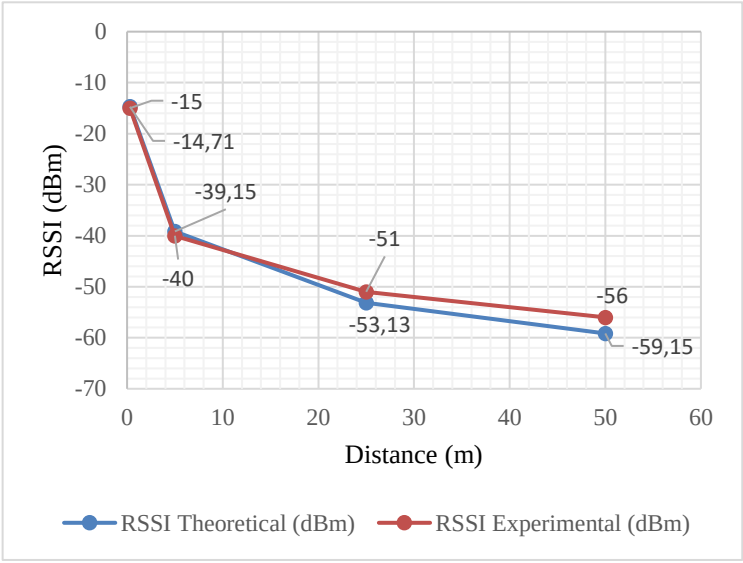

Figure 25. Theoretical vs. Experimental RSSI Comparison for LoRa

Figure 25 compares the FSPL-based theoretical and experimentally measured RSSI values for LoRa at 433 MHz over increasing distances. Both curves show the same overall attenuation behavior: RSSI decreases sharply at short distances and then declines more gradually at longer ranges, consistent with the logarithmic distance dependence of the FSPL model. At 30 cm, the theoretical RSSI is approximately −14.71 dBm, while the experimental value is close to −15 dBm, indicating very strong agreement at the reference short range. At 5 m, the theoretical value is about −39.15 dBm and the measured RSSI is around −40 dBm, again showing only a minor deviation of roughly 1 dB. At 25 m, the theoretical RSSI is approximately −53.13 dBm, whereas the experimental value is around −51 dBm, meaning the measured signal is slightly stronger than the theoretical baseline by about 2 dB. At 50 m, the theoretical prediction is −59.15 dBm and the experimental measurement is approximately −56 dBm, indicating a larger positive deviation of around 3 dB at the longest distance. Overall, the close alignment between theoretical and experimental LoRa curves suggests that distance-dependent attenuation follows the expected baseline trend, while the small positive deviations in the measurements-particularly at longer distances-can be attributed to indoor multipath effects and constructive reflections that may locally enhance received signal levels.

Distance-based measurements from the first, second, and third experimental scenarios demonstrate that ESP32 experiences a more rapid increase in RSSI loss as distance increases. This behavior follows an approximately linear trend, indicating higher sensitivity to distance in indoor environments. In contrast, LoRa exhibits a slower and more gradual RSSI degradation, with only minor variations observed beyond certain distance thresholds. These findings indicate that ESP32 loses signal strength more rapidly than LoRa as distance increases, supporting the conclusion that LoRa provides more stable long-range indoor communication. The numerical results obtained from the first, second, and third experimental scenarios are presented in Table 1, Table 2, and Table 3, respectively.

Table 1. Results of Experiment 1

Experiment	*Module*	*Distance(m)*	*Environment*	*RSSI(dBm)*
1	ESP32	30 cm	4m diameter, no obstacle, ceiling height 2.40m	-31
1	LoRa RA-02	30 cm	4m diameter, no obstacle, ceiling height 2.40m	-15

Table 2. Results of Experiment 2

https://doi.org/10.53525/jster.1892489

Distance (m)	ESP32 RSSI (dBm)	LoRa RSSI (dBm)	LoRa-ESP32 Difference (dB)
5	-52	-40	12
25	-69	-51	18
50	-72	-56	16

Table 3. Results of Experiment 3

Measurement Point	Distance to Sensor (m)	ESP32 RSSI (dBm)	LoRa RSSI (dBm)	LoRa-ESP32 Difference(dB)
0m(L)	5	-54	-38	16
5m(L)	10	-66	-43	23
10m(L)	15	-67	-57	10
15m(L)	20	-71	-58	13

Table 4. Results of Experiment 4

Obstacle Type	ESP32 RSSI (dBm)	ESP32 Additional Loss (dB)	LoRa RSSI (dBm)	LoRa Additional Loss (dB)
Stainless Steel	-51	20	-26	11
Aluminium Composite	-57	26	-27	12
Double Layer Glass	-37	6	-15	0
Plexiglass	-33	2	-15	0
OSB (Oriented Strand Board)	-32	1	-15	0
Chipboard	-32	1	-15	0
Drywall	-33	2	-15	0

Based on these observations, ESP32 is well suited for short-distance and high-speed communication scenarios, whereas LoRa offers clear advantages for longer distances where signal stability is critical. The results obtained from the third experimental scenario further emphasize this distinction. In the L-shaped corridor configuration, where line-of-sight conditions were partially or completely lost, ESP32 showed a pronounced decrease in RSSI values. LoRa, on the other hand, maintained communication at lower RSSI levels and demonstrated greater resilience under non-line-of-sight conditions, as show in Table 1, Table 2, Table 3.

The fourth experimental scenario focused on evaluating the impact of physical obstacles on signal attenuation. The RSSI results obtained under different obstacle conditions are presented in Table 4. In this experiment, obstacles with dimensions of approximately 45–50 cm were placed between the transmitter and receiver. For both communication technologies, materials with high electrical conductivity resulted in more severe signal attenuation. Stainless steel caused a significant reduction in RSSI values, while aluminium composite materials-consisting of dual aluminium layers with an insulating core-produced attenuation levels comparable to or slightly higher than those observed with stainless steel, as shown in Table 4.

For ESP32 communication, non-metallic obstacles produced relatively small RSSI variations that remained within tolerable limits. In contrast, LoRa communication exhibited minimal sensitivity to most obstacle types, often producing RSSI values similar to those observed in unobstructed conditions. These results highlight the superior penetration capability of LoRa signals in indoor environments containing physical obstructions.

https://doi.org/10.53525/jster.1892489

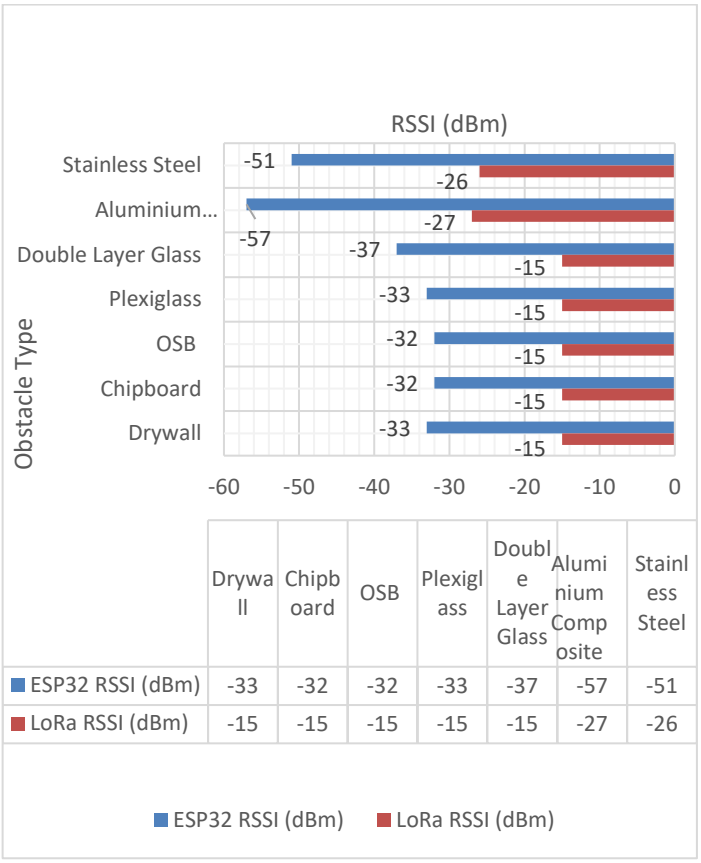

Figure 26. RSSI Variation with Obstacle Materials

Figure 26 presents the measured RSSI values for ESP32 (2.4 GHz) and LoRa (433 MHz) under different obstacle materials placed between the transmitter and receiver, allowing a direct comparison of obstacle-induced attenuation effects. Overall, LoRa maintains consistently higher (less negative) RSSI levels than ESP32 across all tested materials, indicating stronger link robustness under obstructed indoor conditions. For non-metallic obstacles such as drywall, chipboard, OSB, and plexiglass, ESP32 RSSI remains clustered around approximately −32 to −33 dBm, while LoRa stays near −15 dBm, suggesting that these materials introduce limited additional loss within the tested setup. In contrast, conductive materials produce the most pronounced degradation for both technologies. Aluminium composite leads to a major RSSI reduction, with ESP32 dropping to about −57 dBm and LoRa to approximately −27 dBm, while stainless steel also causes substantial attenuation (ESP32 ≈ −51 dBm; LoRa ≈ −26 dBm). Double-layer glass shows a moderate impact compared to metals (ESP32 ≈ −37 dBm), whereas LoRa remains close to its baseline level (≈ −15 dBm). Taken together, the figure highlights that obstacle material properties -particularly electrical conductivity-strongly influence RSSI, and that LoRa exhibits greater resilience than ESP32 in metal-rich or obstacle-dense indoor environments.

Considering all experimental scenarios collectively, the findings indicate that ESP32 provides efficient and reliable communication for short-range and unobstructed indoor applications, whereas LoRa is more suitable for short-, medium-, and long-range scenarios involving physical obstacles. The primary limitation of LoRa communication lies in its lower data rate and payload capacity, which restrict its applicability in high-throughput applications despite its robustness in challenging propagation environments.

V. DISCUSSION

The experimental results can be interpreted primarily through the fundamental differences between the carrier frequencies used by the two communication technologies. In this study, ESP32-based Wi-Fi operates at 2.4 GHz, which lies in the super high frequency (SHF) band, whereas LoRa communication operates at 433 MHz within the ultra-high frequency (UHF) band. Due to the inherent differences in wavelength and propagation characteristics between these frequency bands, a meaningful comparison of distance -and obstacle- related performance becomes possible. Had the two systems operated at similar frequencies, the observed results would likely have converged, limiting the validity of a comparative analysis.

It is well established that higher-frequency signals are generally more sensitive to distance and physical obstructions than lower-frequency signals. This behavior explains why ESP32 communication demonstrates more stable performance at shorter distances but experiences faster signal degradation as distance increases or obstacles are introduced. In contrast, LoRa communication benefits from its lower carrier frequency, which enables improved penetration through walls and other obstacles, as well as more stable propagation over longer distances. The experimental findings obtained under identical indoor conditions confirm this theoretical expectation and provide empirical support for previously reported propagation characteristics [14], [16].

The results further indicate that low-frequency communication protocols exhibit superior robustness against both distance-induced path loss and obstacle-related attenuation. However, this advantage comes with an inherent trade-off. As carrier frequency increases, higher data rates and larger payload capacities become achievable, allowing more information to be transmitted within a given time interval. Consequently, ESP32-based Wi-Fi communication is better suited for applications requiring higher throughput over short and unobstructed distances.

https://doi.org/10.53525/jster.1892489

In contrast, LoRa communication, while offering greater stability and extended range in indoor and outdoor environments, is constrained by lower data rates and smaller payload sizes, necessitating the use of compact data packets for reliable long-distance transmission.

Overall, the findings of this study highlight the importance of frequency selection in indoor wireless system design. The experimental results demonstrate that communication performance is strongly influenced by frequency-dependent propagation behavior, and that the choice between high-frequency and sub-GHz technologies should be guided by application-specific requirements, such as transmission range, obstacle density, and data volume.
The indoor results obtained in this study should be interpreted in relation to the characteristics of the measurement environment. In corridor-based indoor spaces, signal propagation is influenced not only by separation distance but also by wall geometry, reflections from the floor and ceiling, door openings, metallic frames, and directional changes along the propagation path. In particular, in the L-shaped corridor scenario, the transition from line-of-sight to non-line-of-sight propagation introduces additional attenuation mechanisms, such as corner diffraction, partial shadowing, and multipath reception. Under such conditions, the received signal level may not decrease uniformly; instead, local increases or decreases may occur depending on the constructive or destructive interaction of reflected components. In practical deployments, these effects may become even more pronounced in buildings containing elevators, metallic doors, dense furniture, reinforced concrete structures or simultaneously operating wireless systems. Therefore, the results presented here should be regarded as controlled indoor measurements obtained under repeatable test conditions, rather than as universal limits applicable to all indoor environments.

Another important factor underlying the observed performance difference is the spectrum occupancy of the selected operating bands. ESP32-based Wi-Fi operates at 2.4 GHz, one of the most widely used frequency bands in daily life, and is typically shared by routers, mobile devices, smart appliances, and many other short-range wireless systems. As a result, this band is more likely to experience congestion, interference, and channel competition in practical indoor environments. In contrast, the LoRa RA-02 module used in this study was configured to operate at 433 MHz. Compared with the heavily utilized 2.4 GHz band, the 433 MHz band was considerably less occupied in the tested environment, which may have contributed to the more stable reception behavior observed during the experiments. Although other sub-GHz systems may also operate in neighbouring bands, the lower spectrum density at 433 MHz in the present setup provided a practical advantage for obstacle-rich and distance-sensitive indoor transmission.

The reliability of the acquired biomedical and environmental data was also considered during prototype development. For the AD8232-based ECG acquisition unit, preliminary verification was carried out through calibration-oriented comparisons with hospital ECG monitoring outputs and waveform observations. In addition, the pulse calculation logic implemented in the software was refined in light of manual pulse assessment principles discussed with healthcare personnel. For environmental sensing, temperature and humidity values were compared with those obtained from commercially available measurement devices, and calibration adjustments were applied accordingly. It should also be noted that the initial prototype employed a DHT11 sensor; however, because its measurements were not sufficiently stable, the design was revised and the DHT22 sensor was adopted in the final system. Accordingly, the final experimental setup reported in this study is based on the DHT22 configuration.

With respect to data security, access to the transmitter-side interface was controlled at the network access level. To reach the system interface and monitor the transmitted data, the user first had to connect to the device's wireless network, which was protected by password authentication. Accordingly, direct access to the transmitted data was restricted to authorized users who were able to join the protected network. This indicates that a basic access-control mechanism was implemented in the prototype. However, advanced encryption, user-specific authorization, and end-to-end data protection mechanisms were not incorporated in detail in the present system and remain important considerations for future development.

A detailed power-consumption analysis was not carried out in this study. However, practical observations during the experiments indicated that a 10,000 mAh power bank was sufficient to operate the system continuously for approximately 18 hours without depletion. Based on this observation, the average system consumption can be estimated to have remained below the nominal full-capacity limit of the power source, corresponding roughly to an average operating range of less than 2 W under the tested conditions. Although this estimate does not replace direct current and power measurements, it suggests that the prototype can sustain extended operation in practical monitoring scenarios.

https://doi.org/10.53525/jster.1892489

From a real-time monitoring perspective, the proposed system showed stable operation throughout the experiments. Sensor data acquired at the transmitter were packetized, transmitted wirelessly, decoded at the receiver, and displayed on the ST7789 TFT screen in a continuous loop. This enabled real-time observation of both sensor outputs and RSSI values during the measurements. In the ESP32-based configuration, update behavior depended more strongly on connection quality and environmental conditions, whereas in the LoRa-based configuration, communication followed fixed packet intervals. Therefore, the real-time performance of the system should be interpreted not only in terms of raw delay, but also in terms of update regularity and communication continuity. Although detailed timing analyses, such as end-to-end delay, jitter, and packet-level latency, were beyond the scope of this study, the system maintained continuous monitoring functionality throughout the tested indoor scenarios.

This study has several practical limitations that should be acknowledged. First, the experiments were conducted using a single transmitter and a single receiver, and the hardware comparison was limited to the ESP32 and LoRa RA-02 modules. Second, the system architecture was developed within the constraints of the available prototype circuits and budget; therefore, a multi-node communication structure could not be implemented in the present study. In principle, both ESP32- and LoRa-based systems can be extended to support communication among multiple devices by increasing the number of nodes and adapting the circuit topology accordingly. However, the present thesis and article were intentionally limited to a one-to-one communication framework in order to ensure repeatability and enable a controlled comparison.

VI. CONCLUSIONS AND RECOMMENDATIONS

This study presents a comparative evaluation of ESP32-based Wi-Fi and LoRa communication under indoor conditions, focusing on the effects of distance and physical obstacles on RSSI behavior. The experimental results confirm an expected yet important performance difference between the two technologies. While both systems enable reliable indoor data transmission, their effectiveness varies significantly depending on distance, obstacle presence, and application requirements.

The findings indicate that ESP32 provides efficient and stable communication over short distances, particularly in unobstructed environments where higher data rates are desirable. However, as transmission distance increases, ESP32 exhibits a rapid increase in RSSI degradation, leading to weakened link reliability. In contrast, LoRa demonstrates greater tolerance to distance-related path loss, maintaining more stable RSSI values beyond certain distance thresholds. This behavior makes LoRa a more suitable option for medium- and long-range indoor communication scenarios.

Obstacle-based experiments further emphasize this distinction. Materials with high electrical conductivity, such as stainless steel and aluminium composite, caused noticeable signal attenuation for both communication technologies. Nevertheless, LoRa consistently outperformed ESP32 in these conditions, exhibiting superior resilience against obstacle-induced signal loss. The selection of obstacle materials in this study reflects commonly used components in modern buildings, including metallic structural elements, drywall, glass, wood-based furniture materials, and plexiglass. As a result, the experimental outcomes provide practical insights into how different construction materials influence indoor wireless communication performance and guide protocol selection during system design.

Based on these results, ESP32 is recommended for short-range, high-throughput applications within single rooms or unobstructed indoor spaces, whereas LoRa is more appropriate for systems spanning multiple rooms, longer distances or environments with significant physical obstructions. In hybrid system architectures, a combined approach may be advantageous. For example, multiple ESP32 nodes can communicate locally within a networked environment, while LoRa links can be used to transmit aggregated data to remote or obstacle-rich locations, enabling scalable and flexible monitoring systems.

Future work on the proposed system may focus on improving portability, integration, and scalability. Although the socket-based circuit design offered flexibility during the prototyping phase, it also increased the overall device size. More compact modular configurations, integrated battery operation, and expanded data aggregation structures may further enhance the practicality of the system for continuous indoor monitoring applications.

The findings of this study indicate that the indoor performance difference between ESP32-based Wi-Fi and LoRa communication should be interpreted not only in terms of communication range, but also in relation to obstacle sensitivity, operating frequency, transmission structure, and practical monitoring requirements. Under the tested indoor conditions, ESP32 demonstrated satisfactory performance at short distances and in relatively

unobstructed spaces, particularly in cases where faster data exchange and higher throughput are desirable. However, the measurements also showed that ESP32 was more sensitive to increasing distance and to conductive or partially blocking materials, leading to a steeper decline in RSSI.

In contrast, LoRa maintained stronger and more stable reception behavior across both distance-based and obstacle-based scenarios, particularly in the corridor and NLOS measurements. This suggests that LoRa constitutes a more robust solution for indoor monitoring systems operating across multiple rooms, around corners or in the presence of construction materials that may attenuate higher-frequency signals. At the same time, its lower data-rate structure makes it more suitable for compact and periodic monitoring data rather than continuous high-throughput transmission. Future studies may build on the present work by incorporating multi-node architectures, more detailed analyses of delay and packet loss, direct energy-consumption measurements, enhanced data-security mechanisms, and validation under different building and interference conditions.

Author Contributions: CAK – Conceptualization, system design, software development, experimental setup, data collection, data analysis, visualization, and manuscript writing. ROD – Supervision, methodology review, validation, and manuscript review.

Conflict of Interest: The author declares that there is no conflict of interest regarding the publication of this manuscript.

Ethics Committee Approval: This research does not involve human participants, patient data or animal experiments. Therefore, ethics committee approval was not required.

Use of Artificial Intelligence: Artificial intelligence tools were used for language editing, clarity improvement, and structural refinement of the manuscript. All scientific decisions, experimental procedures, data generation, analyses, and interpretations were performed by the author.

REFERENCES

[1] J. Andela, V. Šimák, F. Škultéty, and D. Nemec, "IoT-based data acquisition unit for aircraft and road vehicle," Transportation Research Procedia, vol. 55, pp. 969–976, 2021.

[2] Espressif Systems, "ESP32-WROOM-32D & ESP32- WROOM-32U Datasheet," ver. 2.4, 2023. [Online]. Available: https://www.espressif.com. [Accessed: Jan. 2026].

[3] W. J. Groote Veldman, "Optimizing BLE gateway positioning in aviation industry: An algorithm based on link budget and log-distance path loss," B.Sc. thesis, 2023.

[4] G. Kim, S. Kwon, N. Kim, N. Kim, K. Dhuper, P. Chander, E. T. Matson, and T. Smith, "Power efficient long range drone networking system for UAV detection," in Proc. ICTC 2023, 2023.

[5] P. S. Maria, D. Azmi, A. Zulfadli, and D. Firmansyah, "Robot for underground mining area observation," in Proc. ICECOS 2024, 2024.

[6] V. Oguntosin, C. Chidiuto, and A. Abdulkareem, "Implementation of a LoRa and IoT-based health monitoring and alarm system for the elderly," Engineering Proceedings, vol. 56, 2023.

[7] Shenzhen Ai-Thinker Technology Co., Ltd., "Ra-02 LoRa Module Product Specification," ver. 1.1, 2017. [Online]. Available: http://www.ai-thinker.com. [Accessed: Jan. 2026].

[8] J. H. Rodriguez III, "The design and implementation of soil monitoring systems using UAVs," M.S. thesis, Texas A&M University–Kingsville, Kingsville, TX, USA, 2023.

[9] 7Semi, "SX1278 LoRa RA-02 Breakout Module – User Manual," ver. 1.0, BN-10355, Mar. 26, 2025. [Online]. Available: https://www.7semi.com. [Accessed: Jan. 2026].

[10] Analog Devices, "AD8232: Single-Lead, Heart Rate Monitor Front End," rev. D, 2012–2020. [Online]. Available: https://www.analog.com. [Accessed: Jan. 2026].

[11] SparkFun Electronics, "AD8232 Heart Rate Monitor Reference Design," ver. 1.0, 2014. [Online]. Available: https://www.sparkfun.com. [Accessed: Jan. 2026].

[12] Aosong Electronics Co., Ltd., "DHT22 (AM2302) Digital Temperature and Humidity Sensor Datasheet," 2012–2018. [Online]. Available: http://www.aosong.com. [Accessed: Jan. 2026].

[13] Sitronix Technology Corp., "ST7789VW TFT-LCD Controller/Driver Datasheet," ver. 1.0, Sep. 2017. [Online]. Available: https://www.sitronix.com. [Accessed: Jan. 2026].

[14] Y. Bouazizi, J. A. McCann, F. Benkhelifa, and H. ElSawy, "SF-adaptive duty-cycled LoRa networks: Scalability, reliability, and latency tradeoffs," IEEE Trans. Commun., 2024, doi: 10.1109/TCOMM.2024.3450586.

[15] L. Formanek, M. Kubascik, O. Karpis, and P. Kolok, "Advanced system for remote updates on ESP32-based devices using over-the-air update technology," Computers, vol. 14, no. 12, p. 531, 2025, doi: 10.3390/computers14120531.

[16] T. Sun, Y. Tian, and A. Peng, "Cramer-Rao lower bound of RSS-based fingerprinting positioning assisted by map information," in Proc. 2025 Int. Conf. Indoor Positioning and Indoor Navigation (IPIN), 2025, doi: 10.1109/IPIN66788.2025.11213329.